

# Long-term Monitoring of the Black Hole Binary GX 339–4 in the High/Soft State during the 2010 Outburst with MAXI/GSC

Megumi SHIDATSU,<sup>1</sup> Yoshihiro UEDA,<sup>1</sup> Satoshi NAKAHIRA,<sup>2</sup> Hitoshi NEGORO,<sup>3</sup> Kazutaka YAMAOKA,<sup>4</sup> Mutsumi SUGIZAKI,<sup>2</sup> Kazuo HIROI,<sup>1</sup> Nobuyuki KAWAI,<sup>5</sup> Tatehiro MIHARA,<sup>2</sup> Masaru MATSUOKA,<sup>2,6</sup> Masashi KIMURA,<sup>7</sup> Masaki ISHIKAWA,<sup>8</sup> Naoki ISOBE,<sup>9</sup> Hiroki KITAYAMA,<sup>7</sup> Mitsuhiro KOHAMA,<sup>6</sup> Takanori MATSUMURA,<sup>10</sup> Mikio MORII,<sup>5</sup> Yujin E. NAKAGAWA,<sup>11</sup> Motoki NAKAJIMA,<sup>12</sup> Motoko SERINO,<sup>2</sup> Tetsuya SOOTOME,<sup>2,13</sup> Kousuke SUGIMORI,<sup>5</sup> Fumitoshi SUWA,<sup>3</sup> Takahiro TOIZUMI,<sup>5</sup> Hiroshi TOMIDA,<sup>6</sup> Yohko TSUBOI,<sup>10</sup> Hiroshi TSUNEMI,<sup>7</sup> Shiro UENO,<sup>6</sup> Ryuichi USUI,<sup>5</sup> Takayuki YAMAMOTO,<sup>2,3</sup> Kyohei YAMAZAKI,<sup>10</sup> and Atsumasa YOSHIDA,<sup>4</sup>

<sup>1</sup>*Department of Astronomy, Kyoto University, Oiwake-cho, Sakyo-ku, Kyoto 606-8502*  
*shidatsu@kusastro.kyoto-u.ac.jp*

<sup>2</sup>*MAXI team, Institute of Physical and Chemical Research (RIKEN), 2-1 Hirosawa, Wako, Saitama 351-0198*

<sup>3</sup>*Department of Physics, Nihon University, 1-8-14 Kanda-Surugadai, Chiyoda-ku, Tokyo 101-8308*

<sup>4</sup>*Department of Physics and Mathematics, Aoyama Gakuin University,  
5-10-1 Fuchinobe, Chuo-ku, Sagamihara, Kanagawa 252-5258*

<sup>5</sup>*Department of Physics, Tokyo Institute of Technology, 2-12-1 Ookayama, Meguro-ku, Tokyo 152-8551*

<sup>6</sup>*ISS Science Project Office, Institute of Space and Astronautical Science (ISAS), Japan Aerospace Exploration Agency (JAXA), 2-1-1 Sengen, Tsukuba, Ibaraki 305-8505*

<sup>7</sup>*Department of Earth and Space Science, Osaka University, 1-1 Machikaneyama, Toyonaka, Osaka 560-0043*

<sup>8</sup>*School of Physical Science, Space and Astronautical Science, The graduate University for Advanced Studies (Sokendai), Yoshinodai 3-1-1, Chuo-ku, Sagamihara, Kanagawa 252-5210*

<sup>9</sup>*Institute of Space and Astronautical Science (ISAS), Japan Aerospace Exploration Agency (JAXA), 3-1-1 Yoshino-dai, Chuo-ku, Sagamihara, Kanagawa 252-5210*

<sup>10</sup>*Department of Physics, Chuo University, 1-13-27 Kasuga, Bunkyo-ku, Tokyo 112-8551*

<sup>11</sup>*Research Institute for Science and Engineering, Waseda University, 17 Kikui-cho, Shinjuku-ku, Tokyo 162-0044*

<sup>12</sup>*School of Dentistry at Matsudo, Nihon University, 2-870-1 Sakaecho-nishi, Matsudo, Chiba 101-8308*

<sup>13</sup>*Department of Electronic Information Systems, Shibaura Institute of Technology,  
307 Fukasaku, Minuma, Saitama, Saitama 337-8570*

(Received ; accepted )

## Abstract

We present the results of monitoring the Galactic black hole candidate GX 339–4 with the Monitor of All-sky X-ray Image (MAXI) / Gas Slit Camera (GSC) in the high/soft state during the outburst in 2010. All the spectra throughout the 8-month period are well reproduced with a model consisting of multi-color disk (MCD) emission and its Comptonization component, whose fraction is  $\leq 25\%$  in the total flux. In spite of the flux variability over a factor of 3, the innermost disk radius is constant at  $R_{\text{in}} = 61 \pm 2$  km for the inclination angle of  $i = 46^\circ$  and the distance of  $d = 8$  kpc. This  $R_{\text{in}}$  value is consistent with those of the past measurements with Tenma in the high/soft state. Assuming that the disk extends to the innermost stable circular orbit of a non-spinning black hole, we estimate the black hole mass to be  $M = 6.8 \pm 0.2 M_\odot$  for  $i = 46^\circ$  and  $d = 8$  kpc, which is consistent with that estimated from the Suzaku observation of the previous low/hard state. Further combined with the mass function, we obtain the mass constraint of  $4.3 M_\odot < M < 13.3 M_\odot$  for the allowed range of  $d = 6 - 15$  kpc and  $i < 60^\circ$ . We also discuss the spin parameter of the black hole in GX 339–4 by applying relativistic accretion disk models to the Swift/XRT data.

**Key words:** accretion, accretion disks — black hole physics — stars: individual(GX 339–4) — X-rays: binaries

## 1. Introduction

Black hole binaries (BHBs) exhibit various types of X-ray spectra according to their “state”, which is mainly determined by the mass accretion rate (see e.g., Done et al. 2007 for a recent review). Typically, at low luminosities, they stay in the “low/hard state”, in which the spectrum

is well reproduced by a power law with a photon index of  $\Gamma \simeq 1.7$  and an exponential cutoff at  $\sim 100\text{--}200$  keV. In this state, the accretion disk is likely truncated (e.g., Shidatsu et al. 2011) and its inner part is supposed to be surrounded by hot corona responsible for Comptonization, although the interpretation is still in debate (e.g., Miller et al. 2006). When a transient BHB undergoes an outburst,

it often makes transition from the low/hard state to the “high/soft state”, through the “intermediate state”, after the rapid increase of the luminosity.

The X-ray spectra of BHBs in the high/soft state are well described by a Multi-Color Disk (MCD) model (Mitsuda et al. 1984) accompanied with a small power law with a photon index of  $\Gamma \sim 2\text{--}2.5$  (Done et al. 2007; McClintock & Remillard 2006). A well accepted picture of this state is that the optically thick, geometrically thin disk (so-called the standard disk; Shakura & Sunyaev 1973) is extended down to the innermost stable circular orbit (ISCO). This is strongly supported by the fact that the innermost disk radius estimated from the temperature and luminosity of the MCD model is found to be remarkably constant over a wide luminosity range for a BHB in the high/soft state (e.g., Ebisawa et al. 1994). Since the ISCO depends only on the black hole mass and spin, the MCD parameters can give a constraint on the black hole mass for an assumed spin if the distance and inclination are obtained (e.g., Dotani et al. 1997 for Cyg X-1), independently from the mass function derived from the orbital motion.

X-ray monitoring observations of BHBs during their outbursts give important information on the evolution of the accretion disk as a function of mass accretion rate. In 2009 September, the Monitor of All-sky X-ray Image (MAXI; Matsuoka et al. 2009) on the International Space Station (ISS) started its operation. One goal of the MAXI mission is to detect new transients including BHBs (e.g., Nakahira et al. 2010) and monitor them as well as known X-ray transients with unprecedented sensitivities. In fact, MAXI has detected several outbursts of new BHBs (e.g., MAXI J1659–152, Negoro et al. 2010a; MAXI J1543–564, Negoro et al. 2010b) for about 1.5 years. In addition, MAXI gives us a unique opportunity provides data to study the X-ray spectra of BHBs continuously over a period from the onset of an outburst to its fading phase.

GX 339–4 is a well known Galactic BHB discovered in early 1970s, although its binary-system parameters have not been firmly determined because of the faint magnitude of the companion star. Hynes et al. (2003) estimate the mass function of GX 339–4 to be  $(5.8 \pm 0.5)M_{\odot}$  ( $2.0M_{\odot}$  at a 95% confidence lower limit) from high-resolution optical spectroscopy. Shidatsu et al. (2011) have summarized all available constraints on the distance  $d$  and inclination  $i$  from various observations. The absence of eclipse places a limit of inclination as  $i \lesssim 60^{\circ}$  (Cowley et al. 2002). A tighter constraint,  $i = 46^{\circ} \pm 8^{\circ}$ , is derived by Shidatsu et al. (2011) from the Suzaku spectra in 2009 March in the low/hard state. The distance is constrained by Hynes et al. (2004) to be  $6 < d < 15$  kpc from the structure of the Na D line, and Zdziarski et al. (2004) suggest  $d = 8 \pm 1$  kpc from the apparent radius of the secondary low-mass star.

In 2010 April, GX 339–4 underwent an outburst, and a hard-to-soft transition was observed (Motta et al. 2010). This source was almost continuously observed with MAXI during the outburst. In this paper, we report the first results of the spectral analysis of the MAXI Gas Slit Camera

(GSC; Mihara et al. 2011) during the high/soft state after the transition, with a primary purpose to constrain the black hole mass from the X-ray data. We compare the results with those from three Swift/XRT observations performed simultaneously. We also attempt to estimate the spin parameter of the black hole in GX 339–4 by applying relativistic disk models to the Swift/XRT data. In Section 2, we describe the observations and data reduction of the MAXI/GSC and Swift/XRT data. These results are given in Section 3. We summarize and discuss the results in Section 4. The spectral fit is performed on XSPEC version 12.6.0q. The quoted errors refer to 90% confidence ranges for a single parameter.

## 2. Observation and Data Reduction

### 2.1. Monitoring with MAXI/GSC

In this paper, we only use the GSC data, which covers the energy band of 2–30 keV, considering its wider field-of-view (FoV) and much larger collecting area than the Solid-state Slit Camera on MAXI (Tomida et al. 2011, Tsunemi et al. 2010). The GSC is composed of 12 position-sensitive proportional counters with 6 carbon anodes in each, although four counters has not been operated since 2010 March due to hardware trouble by discharge events.

GX 339–4 entered into a new outburst phase in 2010 January (Yamaoka et al. 2010), and returned to a quiescent state in 2011 March (Russell et al. 2011). This outburst was almost continuously monitored by MAXI/GSC. Figure 1 shows the GSC light curves of GX 339–4 in the energy ranges of 2–4 keV (soft band), 4–10 keV (medium band), and 10–20 keV (hard band)<sup>1</sup>. The Swift/BAT light curve in the 15–50 keV band and hardness ratio between the medium and soft bands of the GSC are also plotted. There are data gap in the MAXI/GSC light curves on MJD 55294–55308 because the source was located close to the direction of the rotation axis of the ISS and was out of the GSC field-of-views. The total X-ray luminosity most likely reached its peak during the period. We find that GX 339–4 stayed in the low/hard state until MJD 55294, showing a power-law-like spectrum with a photon index of  $\approx 1.7$ . In this paper, we concentrate on the data taken during the period between MJD 55310 and 55550, which roughly correspond to the flux peak in the total band and the end of the outburst, respectively. As shown in Figure 1, the source flux in the hard band during MJD 55345–55550 was as small as that before the outburst, indicating that it had been stayed in the high/soft state during the period.

### 2.2. Data Reduction

We extract GSC data from the event files processed with the MAXI standard analysis software described in Sugizaki et al. (2011) and Nakahira et al. (2011), and include only data obtained with the GSC counters operated with the nominal high voltage (1650 V). We exclude events

<sup>1</sup> GSC light curves of about 250 other X-ray sources are available at <http://maxi.riken.jp>

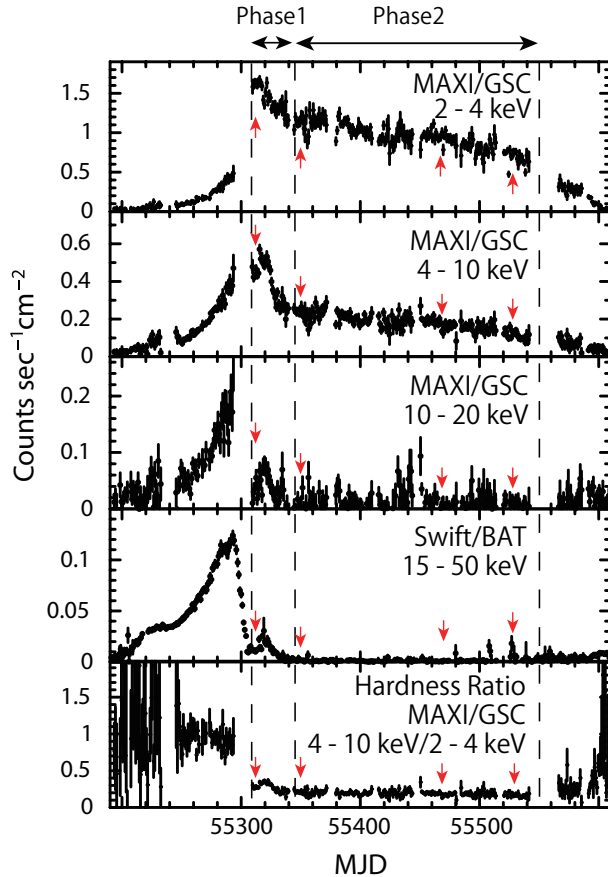


**Fig. 1.** From top to bottom, light curves of GX 339–4 in the 2–4 keV, 4–10 keV, and 10–20 keV bands obtained with MAXI/GSC, that in the 15–50 keV band obtained with Swift/BAT, and hardness ratio between the MAXI/GSC 4–10 keV and 2–4 keV bands. The arrows indicate the periods for the sample spectra shown in Figure 3.

detected by two carbon anodes #1 and #2 in all the counters whose responses have relatively large calibration uncertainties at present (Sugizaki et al. 2011). We extracted the source photons from a region of a circle centered at the target position with a radius of 1.5 deg, and that for the background from a circle with a radius of 3.3 deg excluding a region within 2.0 deg from the target. The image of extracted data is presented in Figure 2, where the regions for source and background are overlaid. We remove the data obtained by a scan that did not cover the whole source and background regions. It is confirmed that the energy response of the GSC is quite reliable within these selection criteria, from an extensive calibration using the Crab nebula (Nakahira et al. 2011). After the data screening, we accumulate the spectra every 3 days in MJD 55310–55344 and every week in MJD 55345–55550, considering the variability of the X-ray fluxes as shown in Figure 1.

### 2.3. Swift/XRT observation and Data Reduction

Swift performed three pointing observations of GX 339–4 on MJD 55352, 55359, and 55366 (corresponding to 2010 June 5, 12, and 19). To check the consistency with

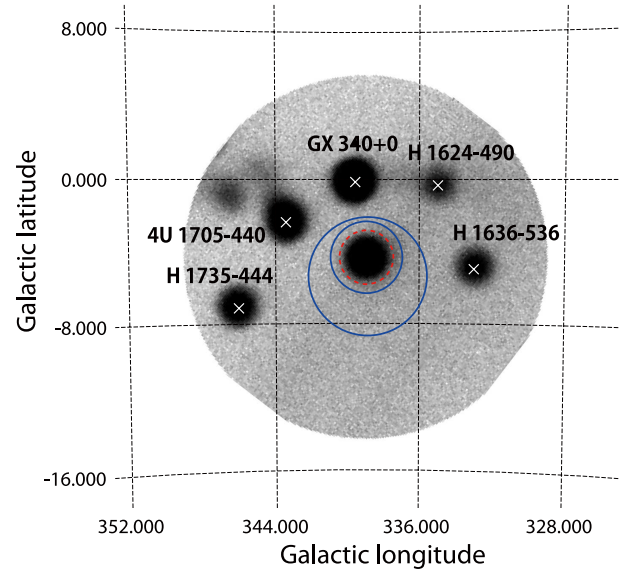


**Fig. 2.** The MAXI/GSC image integrated from MJD 55350 to MJD 55500. The event extraction region of the source is plotted with the red dashed circle, while that of the background corresponds to the area between the two blue circles (solid line).

the MAXI spectra, we also analyze the Swift/XRT data. These observations were all performed in the Windowed Timing (WT) mode (1-dimensional imaging) to avoid pile-up. The net exposures were 1.2, 1.3, and 1.0 ksec, respectively.

We reduce the Swift/XRT archival data with the standard pipeline script `xrtpipeline` provided in the HEASoft analysis package version 6.10. The source events are extracted from a box region of 40 pixels (along DETX coordinate)  $\times$  30 pixels whose center is located at the target position. A 80 pixel  $\times$  30 pixel box is chosen for the background area. In spite of WT mode adopted in these observations, the data still suffer from pile-up as reported by Yan & Yu (2011). Thus, we exclude the events in the “core” region of the source area, a rectangular region of 6 pixels  $\times$  30 pixels centered at the target.

The spectra are extracted with XSELECT version 2.4b. We utilize the response matrix file, `swxwt0to2s6.20070901v012.rmf` in the Swift Calibration Database (CALDB) provided on 2011 February 9. The ancillary response files for the three epochs are created with the tool `xrtmkarf` by using the exposure files produced in the pipeline processing. We add a 3% systematic error to each spectral bin to include possible calibration uncertainties.

### 3. Analysis and Results

We uniformly fit all the MAXI/GSC and Swift/XRT spectra to a partially Comptonized multi-color-disk blackbody (MCD) model with an interstellar absorption. We adopt the `diskbb` model (Mitsuda et al. 1984) for the MCD and the `simpl` model (Steiner et al. 2009) for Compton scattering. The `simpl` model is an empirical

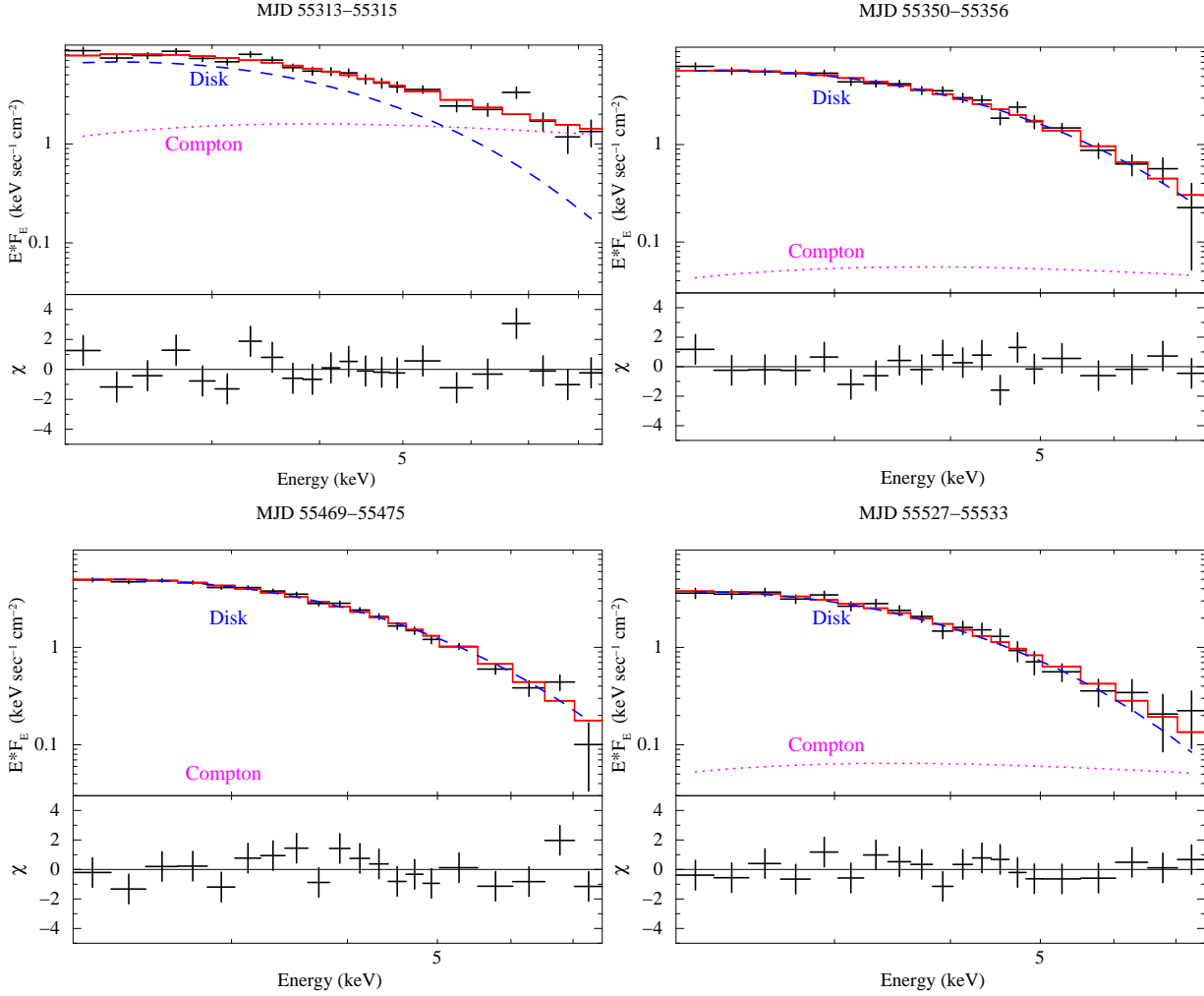


**Fig. 3.** MAXI/GSC time-averaged spectra of GX 339–4 unfolded with the response in the  $\nu F_\nu$  form (crosses, black), extracted from the data of MJD=55313–55315 (top left), 55350–55356 (top right), 55469–55475 (bottom left), and 55527–55533 (bottom right). The best-fit `simpl*diskbb` model is overplotted (solid, red). The contributions from the MCD (dashed, blue) and its Comptonization components (dot, magenta) are separately plotted. The residuals of the fit are shown in the lower panel in units of  $\chi$ . To plot the direct disk and Comptonized components separately, we here represent the model with the form `simpl*diskbb+diskbb`, where the scattered fraction of `simpl` is fixed at 1 and the normalization ratio of the first component to the second one is set to the best-fit scattered fraction.

convolution model that converts a given fraction of the incident spectrum into a power law shape with a photon index  $\Gamma$ . Because of the poor statistics in the hard X-ray ( $> 10$  keV) band, we cannot constrain the photon index of the `simpl` model. Therefore, we fix it at  $\Gamma = 2.5$ , as a typical value for the hard tail of BHs in the high/soft state (McClintock & Remillard 2006). Fitting with a convolution model requires extending the energy range. We set it to 0.01–1000 keV. We use the `phabs` model as the interstellar absorption. The column density is fixed to  $N_{\text{H}} = 0.5 \times 10^{22} \text{ cm}^{-2}$  (Méndez & van der Klis 1997; Kong et al. 2000) for the fit of MAXI/GSC data, while left free for that of Swift/XRT, since the XRT has a sensitivity down to  $\sim 0.4$  keV. The model is expressed as `phabs*(simpl*diskbb)` in the XSPEC terminology. The free parameters of the continuum is three in total, the innermost temperature and normalization of the MCD

component, and the Comptonized fraction in the `simpl` model.

We obtain acceptable fits from all the spectra in terms of  $\chi^2$ . Figures 3 and 4 display examples of the MAXI/GSC and Swift/XRT spectra, respectively, in the  $\nu F_\nu$  form unfolded with the energy response. The best-fit model is overplotted on the data, and the residuals in units of  $\chi$  are shown in the lower panels. The resulting parameters are listed in Table 1. The fraction of the Comptonized component is found to be small ( $\leq 25\%$ ) over the entire periods, indicating that GX 339–4 stayed in the high/soft state, not in the intermediate (or very high) state characterized by a strong Compton component. As shown in Table 1, the absorption column density obtained from the Swift/XRT spectra,  $\approx 0.45 \times 10^{22} \text{ cm}^{-2}$ , is somewhat smaller than  $0.5 \times 10^{22} \text{ cm}^{-2}$  adopted for the spectral fits to the MAXI/GSC spectra, but we confirm that the best-

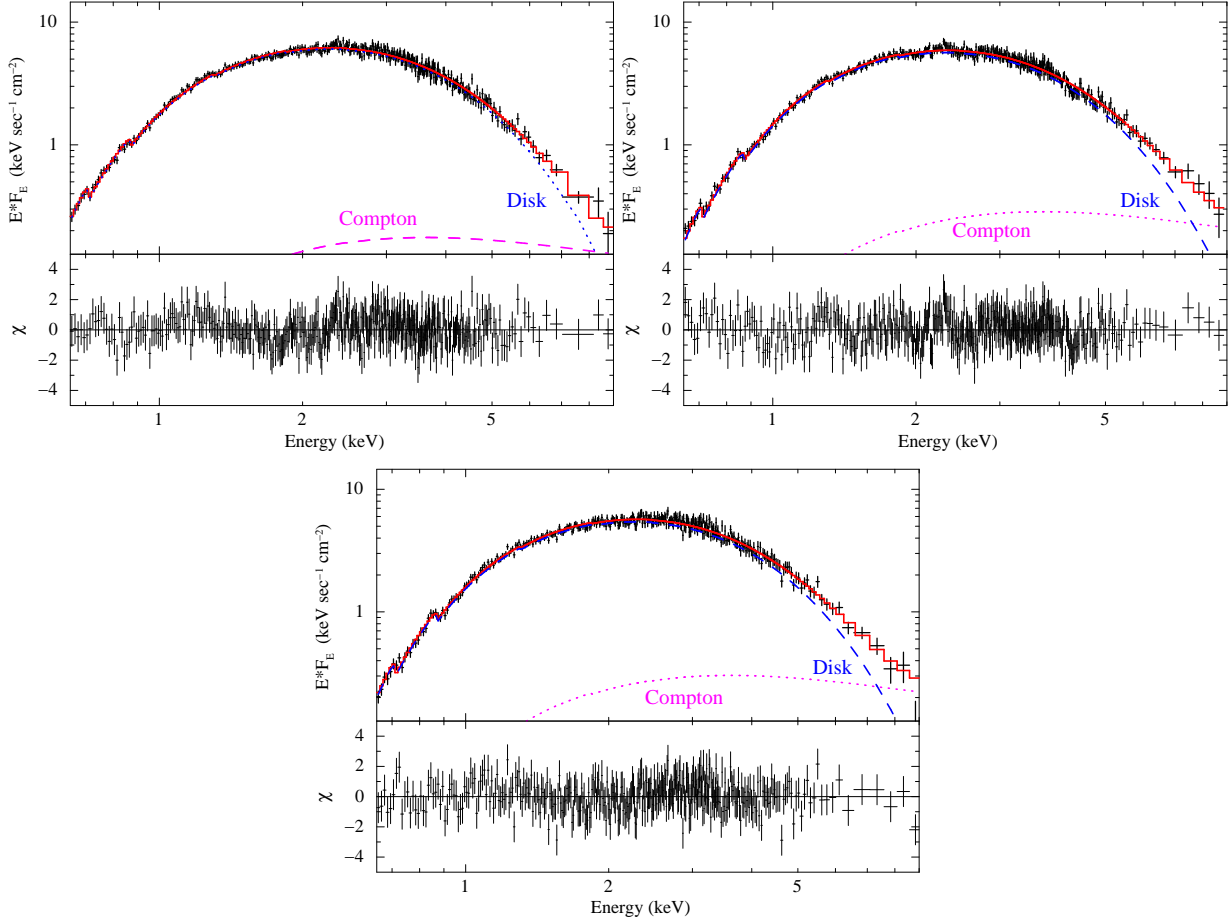


**Fig. 4.** Swift/XRT spectra unfolded with the response in the  $\nu F_\nu$  form (crosses, black), observed on MJD=55352 (top left), 55359 (top right), and 55366 (bottom). The best-fit `simpl*diskbb` model is overplotted (solid, red) with separate contributions from the MCD (dashed, blue) and its Comptonization component (dot magenta). The residuals are shown in the lower panel in units of  $\chi$ .

**Table 1.** Best-fit parameters of the MCD model.

instrument	MJD	$N_{\text{H}}$ ( $10^{22} \text{ cm}^{-2}$ )	$T_{\text{in}}$ (keV)	Compton Fraction (%)	$R_{\text{in}}$ (km)	$\chi^2/\text{d.o.f}$
MAXI/GSC	55313–55315	0.5 (fix)	$0.80^{+0.07}_{-0.08}$	$17^{+7}_{-6}$	$67^{+13}_{-16}$	23/20
MAXI/GSC	55350–55356	0.5 (fix)	$0.78^{+0.06}_{-0.04}$	< 5	$60^{+12}_{-6}$	11/20
MAXI/GSC	55469–55475	0.5 (fix)	$0.75^{+0.01}_{-0.02}$	< 1	$60^{+4}_{-3}$	19/20
MAXI/GSC	55527–55533	0.5 (fix)	$0.70^{+0.05}_{-0.06}$	< 5	$61^{+15}_{-10}$	9/17
Swift/XRT	55352	$0.426^{+0.005}_{-0.007}$	$0.806^{+0.008}_{-0.009}$	$1.9^{+0.8}_{-0.7}$	$57 \pm 1$	317/391
Swift/XRT	55359	$0.486 \pm 0.008$	$0.812 \pm 0.009$	$3.3^{+0.8}_{-0.9}$	$55 \pm 1$	347/391
Swift/XRT	55366	$0.444^{+0.006}_{-0.008}$	$0.796^{+0.009}_{-0.006}$	$3.6^{+0.8}_{-0.9}$	$56^{+1}_{-4}$	301/341

fit inner disk radius derived from the MAXI/GSC data are unchanged ( $< 1\%$ ) within the 90% confidence errors even when we fix  $N_{\text{H}} = 0.4 \times 10^{22} \text{ cm}^{-2}$ .

Figure 5 plots the evolution of the Comptonized fraction (top panel), innermost temperature of the MCD component (second), inner disk radius (third), and 2–20 keV band flux (bottom). The innermost radius is derived from the normalization of the MCD component, by applying the combined correction factor of 1.18 for the stress-free boundary condition ( $\xi = 0.41$ ; see Kubota et al. 1998) and the color hardening factor ( $\kappa = 1.7$ , Shimura & Takahara 1995). Here we adopt the inclination angle  $i = 46^\circ$  from the Shidatsu et al. (2011), and assume the distance  $d = 8$  kpc as the most reasonable estimate (Zdziarski et al. 2004). It can be noticed that the inner radius stayed almost constant at  $\sim 60$  km, while the temperature gradually decreased with time according to the flux change. The constancy of the radius is consistent with the generally accepted picture of the high/soft state in which the standard disk is always extending to the ISCO. Figure 6 plots the disk bolometric luminosity  $L_{\text{disk}}$  in terms of Eddington luminosity  $L_{\text{Edd}}$  versus the inner temperature  $T_{\text{in}}$  obtained from the MCD fit of the MAXI/GSC data. We assume the distance, inclination, and black hole mass to be  $d = 8$  kpc,  $i = 46^\circ$ , and  $6.8M_{\odot}$ , respectively. As shown in Figure 6, the data points roughly follow a simple relation  $L_{\text{disk}} \propto T_{\text{in}}^4$ , which is expected from MCD emission with a constant innermost radius.

To check the effects on the estimated inner disk radius by the assumed geometry of the Comptonizing corona, we also calculate  $R_{\text{in}}$  from the MAXI/GSC spectra on MJD 55325–55327 as representative data, assuming that the Comptonized emission modelled by `simpl` is isotropic. We use the equation of photon conservation expressed as follows (Kubota & Makishima 2004):

$$F_{\text{disk}}^p + F_{\text{thc}}^p 2 \cos i = 0.0165 \left[ \frac{r_{\text{in}}^2 \cos i}{(D/10 \text{ kpc})^2} \right] \left( \frac{T_{\text{in}}}{1 \text{ keV}} \right)^3 \text{ photons s}^{-1} \text{ cm}^{-2}. \quad (1)$$

where  $F_{\text{disk}}^p$  and  $F_{\text{thc}}^p$  are the unabsorbed 0.01–100 keV photon flux from the disk and Comptonized components, respectively. Taking into account the correction factor of 1.18 (Kubota et al. 1998), we obtain the inner disk radius of  $R_{\text{in}} = 64_{-5}^{+6}$  km. It is consistent with that calculated from the normalization of the MCD component (as plotted in Figure 5) by assuming disk-like geometry for the Comptonized emission. Also, we find that these results are not changed when we replace `simpl` with `nthcomp`, a more physical model for thermal Comptonization. Hence, we can ignore the systematic uncertainties due to Comptonization in discussing the inner disk radius.

The real disk spectrum around a black hole, however, should deviate from the MCD spectrum due to the inner boundary condition, and to relativistic effects including gravitational redshift, beaming, and light bending, which become particularly important for a rapidly spinning black hole. Precise measurement of the spectral

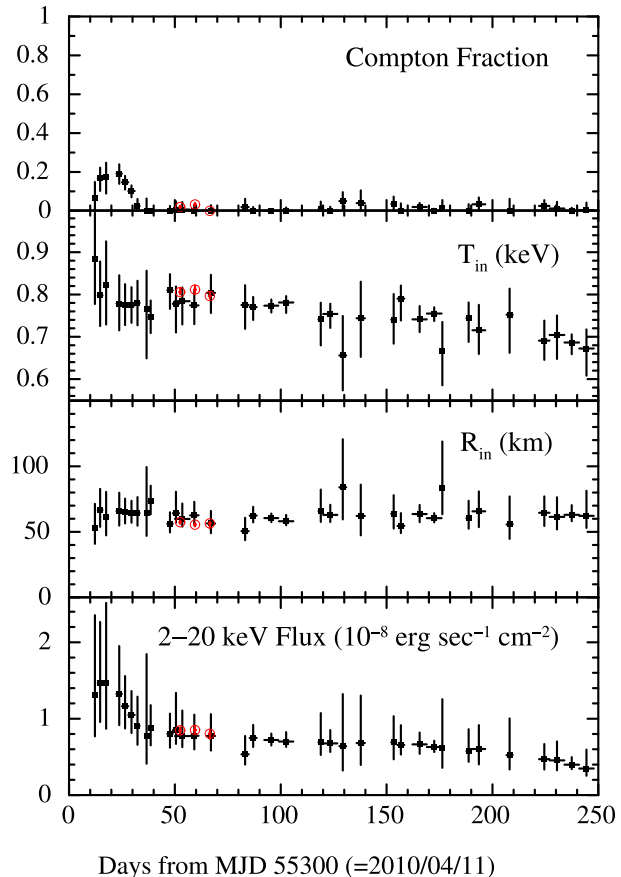


**Fig. 5.** Evolution of Comptonized fraction in the `simpl` model (top), innermost temperature  $T_{\text{in}}$  (second), inner disk radius  $R_{\text{in}}$  estimated from the normalization of `diskbb` component (third), and unabsorbed 2–20 keV flux (bottom). The MAXI and Swift results are plotted in black (filled square) and red (open circle), respectively.

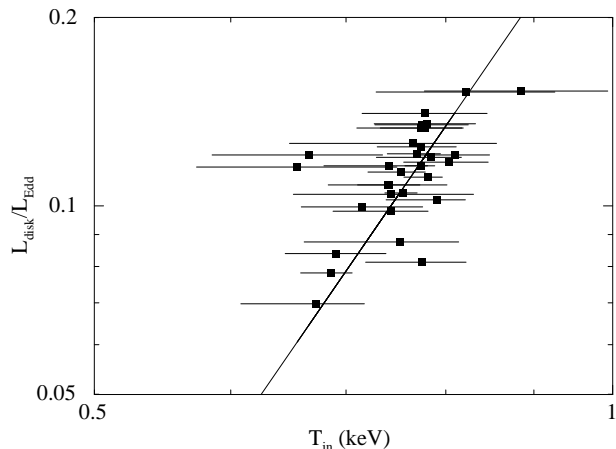


**Fig. 6.** The luminosity-temperature relation of the disk component of GX 339–4 in the high/soft obtained from the MAXI/GSC data with the MCD fit. The data points are fitted by a power-law with  $L_{\text{disk}} \propto T_{\text{in}}^4$  (solid line).

**Table 2.** Best-fit parameters of relativistic disk models from the Swift/XRT data on MJD 55359.

model	$N_{\text{H}}$ ( $10^{22} \text{ cm}^{-2}$ )	$a$	$i$ (deg)	$d$ (kpc)	$M_{\text{BH}}$ ( $M_{\odot}$ )	$\dot{M}$ ( $10^{18} \text{ g s}^{-1}$ )	$L_{\text{disk}}/L_{\text{Edd}}$	Compton Fraction (%)	$\chi^2/\text{d.o.f}$
<b>kerrbb*</b>	$0.509^{+0.009}_{-0.008}$	$< 0.05$	$38^{+2}_{-0}$	8 (fix)	$4.6^{+0.2}_{-0.1}$	$2.27^{+0.05}_{-0.03}$		$1.9^{+0.5}_{-0.8}$	363/389
<b>bhspec†</b>	$0.530 \pm 0.08$	$< 0.33$	$38^{+5}_{-0}$	8 (fix)	$4.6^{+0.5}_{-0.1}$		$0.226^{+0.004}_{-0.017}$	$3.5^{+0.5}_{-0.6}$	345/389

\* Self-irradiation is not included (rflag=0), and limb-darkening is taken into account (lflag=1). The torque-free inner edge is assumed.

† We fixed  $\log(\alpha) = 0.01$ , where  $\alpha$  is the viscosity parameter in the Shakura & Sunyaev (1973) prescription for the stress  $\tau_{r\phi} = \alpha \times P$  ( $P$  is the total pressure).

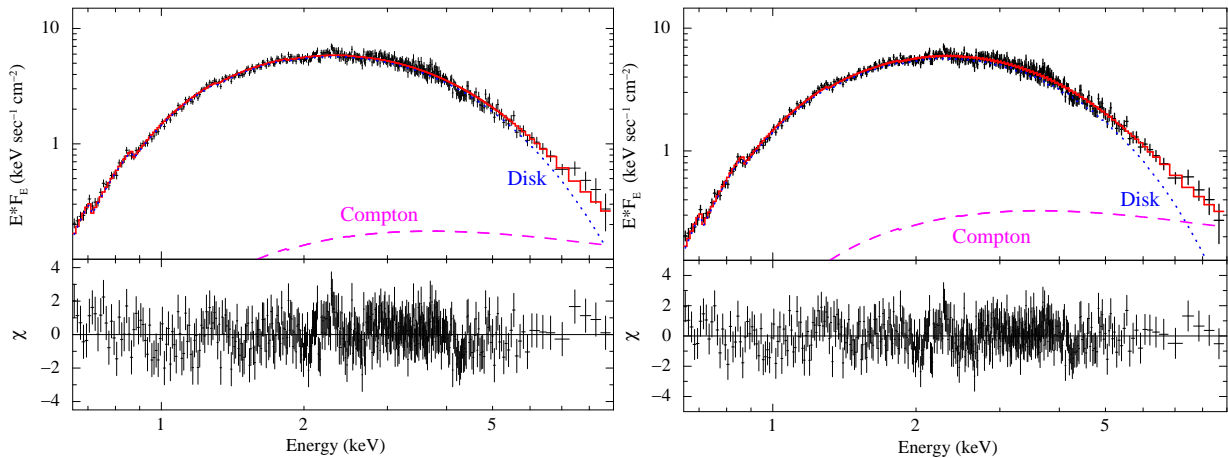


**Fig. 7.** Swift/XRT spectrum on MJD=55359 unfolded with the response in the  $\nu F_{\nu}$  form (crosses, black). The best-fit **simpl\*kerrbb** (left) and **simpl\*bhspec** (right) models are overplotted (solid, red) with separate contributions from the disk emission (dashed, blue) and its Comptonization component (dot magenta). The residuals are shown in the lower panel in units of  $\chi$ .

shape of the disk emission may be used to obtain information on the spin of a black hole even if all system parameters, the black hole mass, distance, and inclination, are not accurately known. With an aim to constrain the spin parameter of GX 339–4, we analyze the Swift/XRT data with the more advanced disk models **kerrbb** (Li et al. 2005) and **bhspec** (Davis et al. 2005) instead of **diskbb**. Both codes relativistically compute the spectrum from a geometrically-thin accretion disk around a spinning black hole with an arbitrary spin parameter  $a \equiv cJ/GM^2$ , where  $M$  and  $J$  are the mass and angular momentum of the black hole,  $c$  the speed of light, and  $G$  the gravitational constant (Shapiro & Teukolsky 1986). Similarly to the previous MCD fit, the disk emission is convolved with **simpl** to represent the Comptonized component.

We fit the Swift/XRT spectrum observed on MJD 55359 as representative data with the model expressed as **phabs** × (**simpl\*kerrbb**) or **phabs** × (**simpl\*bhspec**). The distance is fixed at  $d = 8$  kpc, while the spin parameter and mass accretion rate (**kerrbb**) or Eddington ratio (**bhspec**) are left as free parameters. We assume  $a \geq 0$  (i.e., the spin direction of the black hole is the same as that of the accretion disk). In the **kerrbb** model, the spectral hardening factor is fixed at 1.7, and zero torque is assumed at the inner edge of the disk. First, we fix the inclination at  $i = 46^\circ$  (the best estimate of Shidatsu et al. 2011), and the black hole mass at  $M = 15.6M_{\odot}$  calculated from the mass function of  $f(M) = 5.8M_{\odot}$  (Hynes et al. 2003). The fit is

acceptable ( $\chi^2/\nu = 395/391$ ), and the spin parameter is constrained to be  $a = 0.94^{+0.02}_{-0.01}$  (in the case of the **kerrbb** model). Next, considering the uncertainty in the mass function ( $f(M) > 2M_{\odot}$ ), we make both black hole mass and inclination free parameters. The inclination is allowed to vary only in the range of  $38^\circ \leq i \leq 54^\circ$  (Shidatsu et al. 2011). The fitting results are shown in Table 2 and Figure 7. The fit is significantly improved ( $\chi^2/\nu = 363/389$ ) compared with the previous fit where  $M$  and  $i$  are fixed. We obtain the spin parameters  $a < 0.05$  or  $a < 0.33$  with the black hole mass of  $M = 4.6^{+0.2}_{-0.1}M_{\odot}$  or  $M = 4.6^{+0.5}_{-0.1}M_{\odot}$  from the **kerrbb** or **bhspec** fit, respectively. This result that a small value of the  $a$  parameter is favored is not changed even when the energy band below 1 keV is ignored to avoid any systematic uncertainties in the low energy response, or when a smaller photon index of  $\Gamma = 2.0$  is adopted for the **simpl** model instead of  $\Gamma = 2.5$ . The same trend is also confirmed from the other two Swift/XRT spectra taken on MJD=55352 and 55366.

#### 4. Discussion and Conclusion

We have acquired uniform-quality X-ray spectra of GX 339–4 every 3 or 7 days in the high/soft state during the 2010 outburst from the MAXI/GSC monitoring data. All the spectra are found to be well represented by a partially Comptonized MCD model, from which we are able to estimate the inner disk radius. As shown in Figure 5, the

inner radii obtained from the MAXI/GSC data are consistent with those of the simultaneous Swift/XRT data, which covers a softer energy band in the 0.6–10 keV and is more sensitive to determine the parameters of the MCD component. The consistency between MAXI/GSC and Swift/XRT indicates that our MAXI results are quite reliable, not subject to systematic uncertainties in the responses. The inner radius stayed almost constant over the whole period of 8 months, during which the X-ray flux changed by a factor of 3. This confirms the standard model scenario in the high/soft state that the accretion disk is (stably) extending down to the ISCO.

Our best estimate of the inner disk radius is

$$R_{\text{in}} = (61 \pm 2) \left( \frac{d}{8 \text{ kpc}} \right) \left( \frac{\cos(46^\circ)}{\cos(i)} \right)^{\frac{1}{2}} \text{ km}, \quad (2)$$

which is a weighted average from the MAXI/GSC results over the period from MJD 55310 to MJD 55550. We confirm that this value is consistent with previous measurements using the MCD flux in the high/soft state. In 1983, Makishima et al. (1986) observed GX 339–4 in outburst three times with the Tenma satellite. We find that their estimated inner radius becomes  $59 \pm 1$ ,  $59 \pm 1$ , and  $58 \pm 1$  km for  $i = 46^\circ$  and  $d = 8$  kpc, after correcting for the boundary condition and color hardening factor as described above. Belloni et al. (1999) performed three target-of-opportunity observations of GX 339–4 in the 1998 outburst with RXTE, two of which correspond to the period of the high/soft state. They obtained the inner radius of  $80 \pm 11$  and  $72 \pm 1$  km for  $i = 46^\circ$  and  $d = 8$  kpc. These values are somewhat larger than the Tenma result (Makishima et al. 1986) as well as our MAXI/GSC and Swift/XRT results. The reason is yet unclear and we do not pursue this in our paper.

Assuming that the stable inner disk of a BHB in the high/soft state corresponds to the ISCO, we can estimate the black hole mass from the obtained  $R_{\text{in}}$  value, which is coupled with the spin parameter  $a$ . For a non-spinning black hole, the ISCO correspond to  $6R_g$  ( $R_g$  represents the gravitational radius  $GM/c^2$ ). Using our best estimate on the inner disk radius from the MAXI data,  $61 \pm 2$  (km), we constrain the black hole mass of GX 339–4 to be  $6.8 \pm 0.2 M_\odot$  by assuming  $i = 46^\circ$  and  $d = 8$  kpc in the case of non-spinning black hole. This value is consistent with the constraint of  $M = 4 - 16 M_\odot$  discussed in Section 4 of Shidatsu et al. (2011) based on the comparison of the iron-K line profile and the MCD component from the Suzaku spectra in the low/hard state.

Combined with the mass function  $f(M)$ , defined as

$$f(M) = \frac{M}{\left(1 + \frac{M_c}{M}\right)^2} \sin^3 i \approx M \sin^3 i, \quad (3)$$

where  $M_c$  represents the mass of the companion star, the radius of the ISCO,  $R_{\text{in}} = 61 \pm 2$  (km), constrains the relation between the inclination and distance for an assumed spin parameter  $a$ . In the approximation, we ignore the term  $\frac{M_c}{M}$ , which is less than 0.08 (Zdziarski et al. 2004). The  $f(M)$  value of GX 339–4 was estimated by Hynes

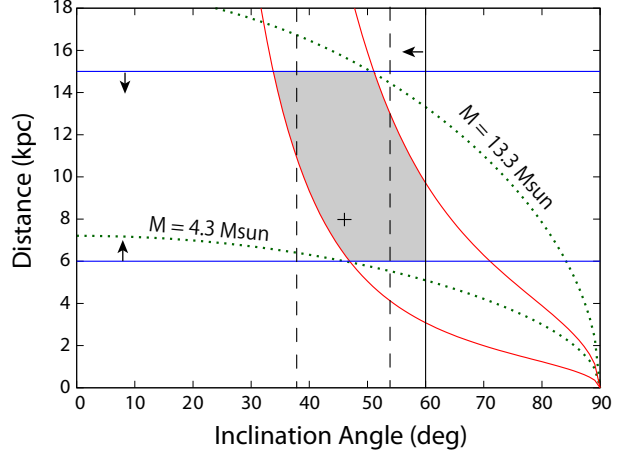


**Fig. 8.** Diagram of constraints on the distance and the inclination angle of GX 339–4. The two solid curves (red) are obtained from our estimate of the inner disk radius  $R_{\text{in}}$  and the mass function  $f(M) = (2.0 - 6.3)M_\odot$ . The spin parameter of  $a = 0$  is assumed. The lower and upper limits on the distance (blue) are taken from by Hynes et al. (2004). The upper limit of the inclination ( $i \leq 60^\circ$ ) from the absence of an eclipse (Cowley et al. 2002) and its 90% confidence region obtained by Shidatsu et al. (2011) from the iron-K line profile are plotted by the solid and dashed lines, respectively. The cross denotes the reference point used for our best estimate of the black hole mass. The constant black-hole mass curves are plotted by dotted green lines for the case of  $M = 13.3M_\odot$  (upper) and  $M = 4.3M_\odot$  (lower).

et al. (2003) to be  $(5.8 \pm 0.5)M_\odot$  ( $2.0 M_\odot$  at a 95% confidence lower limit), which can be converted to a black hole mass (hence the ISCO for an assumed spin) at a given inclination angle. By equating it with the equation (2), we can determine the distance. The gray region in Figure 8 shows the constraints on the inclination and distance obtained in this way within the allowed range of  $f(M) = (2.0 - 6.3)M_\odot$ , assuming  $a = 0$  (i.e.,  $R_{\text{in}} = 6R_g$ ). Here only the  $i < 60^\circ$  region is considered, which comes from the absence of an eclipse (Cowley et al. 2002), and the distance is limited to be  $6 \text{ kpc} < d < 15 \text{ kpc}$  from the structure of NaD line (Hynes et al. 2004). A relation between the inclination and distance corresponding to a given black hole mass can be derived from the equation (2), where  $a = 0$  is assumed. As shown in dotted green lines in Figure 8, the allowed upper and lower limits of the black hole mass in the grey area obtained from this relation are  $13.3 M_\odot$  and  $4.3 M_\odot$ , which happens at the intersections between the  $d = 15$  kpc line and  $f(M) = 6.3M_\odot$  curve, and that between the  $d = 6$  kpc line and the  $f(M) = 2.0M_\odot$  one, respectively. We also plot the constraint of  $i = (46 \pm 8)^\circ$  (within dashed lines) obtained by Shidatsu et al. (2011) from the analysis of the iron-K line profile. Thus, the allowed region in the  $i$  and  $d$  space derived from  $R_{\text{in}}$  and  $f(M)$  for the case of  $a = 0$  is well compatible with all these previous constraints, including the point of  $i = 46^\circ$  and  $d = 8$  kpc as the best estimate.

For more detailed discussion, we need relativistic disk models since the MCD model is only a simple approx-

imation of the disk spectrum (see e.g., Kubota et al. 2010). The analysis of high quality X-ray spectra of a BHB in the high/soft state with such models gives us information on the spin parameter of the black hole. Using the Swift/XRT spectrum, we obtain a large spin parameter  $a \approx 0.94$  when the mass and the inclination are fixed at  $M = 15.6M_{\odot}$  at  $d = 8$  kpc and  $i = 46^{\circ}$ , respectively. However, the resultant spin strongly depends on the assumed mass and inclination; Kolehmainen et al. (2011) derived  $a = 0.1 - 0.5$  from the XMM-Newton and RXTE spectra of GX 339–4 in the high/soft state with the `bhspec` model, assuming  $10M_{\odot}$  at  $d = 8$  kpc with an inclination of  $60^{\circ}$ . Thus, tighter determination of the system parameters of GX 339–4 than that available at present is necessary to derive a reliable answer.

We have also shown the possibility to constrain the black hole spin from the X-ray continuum emission alone without independent information on the mass. In fact, we find that the quality of the fit is significantly improved when the mass and inclination are left as free parameters, which favors a small value of the spin parameter ( $a < 0.05$  and  $a < 0.33$  with the `kerrbb` and `bhspec` models, respectively). This can be understood because the relativistic broadening of the disk spectrum in GX 339–4 looks less significant than that predicted from a large spin parameter. It must be noted, however, that there remain systematic uncertainties at  $\sim 5\%$  level in the current disk models as discussed by Kolehmainen et al. (2011), which could affect the spectral fitting. Further development of theoretical models reproducing the disk emission would be very useful in this context. Finally, we note that the best-fit black hole mass derived from the `kerrbb` and `bhspec` fits are both  $M \approx 4.6M_{\odot}$  at  $d = 8$  kpc with the spin parameter  $a \simeq 0$  and inclination  $i = 38^{\circ}$ . The mass is  $\sim 30\%$  smaller than that obtained from the same Swift/XRT spectrum with the MCD fit by assuming zero-spin ( $M = 6.8M_{\odot}$  for  $d = 8$  kpc and  $i = 38^{\circ}$ ). This difference should be considered as a systematic error in estimating the black hole mass, which we must bear in mind in the critical discussion with accuracy better than 30% levels.

This work made use of the Swift public data archive. This research was partially supported by the Ministry of Education, Culture, Sports, Science and Technology (MEXT), Grant-in-Aid No.19047001, 20041008, 20244015, 20540237, 21340043, 21740140, 22740120, 23000004, 23540265, and Global-COE from MEXT “The Next Generation of Physics, Spun from Universality and Emergence” and “Nanoscience and Quantum Physics”.

## References

- Belloni, T., Méndez, M., van der Klis, M., Lewin, W. H. G., & Dieters, S. 1999, *ApJ*, 519, L159
- Cowley, A. P., Schmidtke, P. C., Hutchings, J. B., & Crampton, D. 2002, *AJ*, 123, 1741
- Davis S. W., Blaes O. M., Hubeny I., & Turner N. J., 2005, *ApJ*, 621, 372
- Done, C., Gierliński, M., & Kubota, A. 2007, *A&A Rev.*, 15, 1
- Dotani, T., et al. 1997, *ApJ*, 485, L87
- Ebisawa, K., et al. 1994, *PASJ*, 46, 375
- Hynes, R. I., Steeghs, D., Casares, J., Charles, P. A., & O’Brien, K. 2003, *ApJ*, 583, L95
- Hynes, R. I., Steeghs, D., Casares, J., Charles, P. A., & O’Brien, K. 2004, *ApJ*, 609, 317
- Kolehmainen, M., Done, C., & Diaz Trigo, M. 2011 *MNRAS*, 416, 311
- Kong, A. K. H., Kuulkers, E., Charles, P. A., & Smale, A. P. 2000, *MNRAS*, 311, 405
- Kubota, A., Tanaka, Y., Makishima, K., Ueda, Y., Dotani, T., Inoue, H., & Yamaoka, K. 1998, *PASJ*, 50, 667
- Kubota, A., & Makishima, K. 2004, *ApJ*, 601, 428
- Kubota, A., Done, C., Davis, S. W., Dotani, T., Mizuno, T., & Ueda, Y., 2010, *ApJ*, 714, 860
- Li, L.-X., Zimmerman, E. R., Narayan, R., & McClintock, J. E. 2005, *ApJS*, 157, 335
- Makishima, K., Maejima, Y., Mitsuda, K., Bradt, H. V., Remillard, R. A., Tuohy, I. R., Hoshi, R., & Nakagawa, M. 1986, *ApJ*, 308, 635
- Matsuoka, M., et al. 2009, *PASJ*, 61, 999
- McClintock, J. E., & Remillard, R. A. 2006, in *Compact Stellar X-Ray Sources*, ed. W. H. G., Lewin, & M. van der Klis (Cambridge: Cambridge Univ. Press), 157
- Méndez, M., & van der Klis, M. 1997, *ApJ*, 479, 926
- Mihara, T., et al. 2011, *PASJ*, in press
- Miller, J. M., Homan, J., Steeghs, D., Rupen, M., Hunstead, R. W., Wijnands, R., Charles, P. A., & Fabian, A. C. 2006, *ApJ*, 653, 525
- Mitsuda, K., et al. 1984, *PASJ*, 36, 741
- Motta, S., Belloni, T., & Muñoz Darias, T. 2010 *The Astronomer’s Telegram No.2545*
- Nakahira, S., et al. 2010, *PASJ*, 62, L27
- Nakahira, S., et al. 2011, in preparation
- Negoro, H., et al. 2010a, *The Astronomer’s Telegram No.2873*
- Negoro, H., et al. 2010b, *The Astronomer’s Telegram No.3330*
- Russell, D. M., Homan, J., Fridriksson, J. K., Lewis, F., Roche, P., & O’Morain, C. 2011, *The Astronomer’s Telegram No.3383*
- Shakura, N. I., & Sunyaev, R. A. 1973, *A&A*, 24, 337
- Shapiro, S. L., & Teukolsky, S. A. 1986, *Black Holes, White Dwarfs and Neutron Stars: The Physics of Compact Objects (Wiley-VCH)*, 357
- Shidatsu, M., et al. 2011, *PASJ*, in press
- Shimura, T., & Takahara, F. 1995 *ApJ*445, 780
- Steiner, J. F., Narayan, R., McClintock, J. E., & Ebisawa, K. 2009, *PASP*, 121,1279
- Sugizaki, M., et al. 2011, *PASJ*, in press
- Tomida, H., et al. 2011, *PASJ*, 63, 397
- Tsunemi, H., Tomida, H., Katayama, H., Kimura, M., Daikyuji, A., Miyaguchi, K., Maeda, K., & MAXI Team 2010, *PASJ*, 62, 1371
- Yamaoka, K., et al. 2010, *The Astronomer’s Telegram No.2380*
- Yan, Z., & Yu, W. Z. 2011, *arXiv:1104.2785*
- Zdziarski, A. A., Gierliński, M., Mikołajewska, J., Wardziński, G., Smith, D. M., Harmon, B. A., & Kitamoto, S. 2004, *MNRAS*, 351, 791